Journal of Neuroscience Methods 374 (2022) 109581

Contents lists available at ScienceDirect

Journal of Neuroscience Methods

journal homepage: www.elsevier.com/locate/jneumeth

Categorical predictive and disease progression modeling in the early stage of Alzheimer's disease

Carlos Platero

Health Science Technology Group, Technical University of Madrid, Ronda de Valencia 3, 28012 Madrid, Spain

ARTICLE INFO

Keywords:
Alzheimer's disease
Mild cognitive impairment
Longitudinal analysis
Predictive models

ABSTRACT

Background: A preclinical stage of Alzheimer's disease (AD) precedes the symptomatic phases of mild cognitive impairment (MCI) and dementia, which constitutes a window of opportunities for preventive therapies or delaying dementia onset.
New method: We propose to use categorical predictive models based on survival analysis with longitudinal data which are capable of determining subsets of markers to classify cognitively unimpaired (CU) subjects who progress into MCI/dementia or not. Subsequently, the proposed combination of markers was used to construct disease progression models (DPMs), which reveal long-term pathological trajectories from short-term clinical data. The proposed methodology was applied to a population recruited by the ADNI.
Results: A very small subset of standard MRI-based data, CSF markers and cognitive measures was used to predict CU-to-MCI/dementia progression. The longitudinal data of these selected markers were used to construct DPMs using the algorithms of growth models by alternating conditional expectation (GRACE) and the latent time joint mixed effects model (LTJMM). The results show that the natural history of the proposed cognitive decline classifies the subjects well according to the clinical groups and shows a moderate correlation between the conversion times and their estimates by the algorithms.
Comparison with existing methods: Unlike the training of the DPM algorithms without preselection of the markers, here, it is proposed to construct and evaluate the DPMs using the subsets of markers defined by the categorical predictive models.
Conclusions: The estimates of the natural history of the proposed cognitive decline from GRACE were more robust than those using LTJMM. The transition from normal to cognitive decline is mostly associated with an increase in temporal atrophy, worsening of clinical scores and pTAU/Aβ. Furthermore, pTAU/Aβ, Everyday Cognition score and the normalized volume of the entorhinal cortex show alterations of more than 20% fifteen years before the onset of cognitive decline.

1. Introduction

Alzheimer's disease (AD) is the most common neurodegenerative disorder in the elderly. AD is characterized by a progressive loss of cognitive abilities and specific neuropathological alterations. Accumulation of amyloid plaques (Aβ deposition) and neurofibrillary tangles (pathologic tau) in the brain are the main symptoms, which may begin as early as middle age (Hyman et al., 2012). A preclinical stage of AD precedes the symptomatic phases of mild cognitive impairment (MCI) and dementia. Autopsy studies identified the early stages of Aβ and tau pathologies in individuals who were cognitively unimpaired (CU) during life, representing a preclinical stage of AD (Price et al., 2009). The predominant research hypothesis postulates that Aβ precedes and accelerates neocortical tau pathology and, together, these factors precipitate cognitive decline (Nelson et al., 2012).

Many clinical trials and interventions for dementia are focused on the preclinical stage of AD, which constitutes a window of opportunities for prevention therapies or delaying dementia onset. Demonstrating that treatments are effective during the early stage will require understanding of the magnitudes of beta-amyloid and tau pathologies in CU adults (Sperling et al., 2014). However, the relation between Aβ and tau status and cognition in early AD varies widely (Baker et al., 2017; Insel et al., 2019). Therefore, it is critical to understand the course of AD from early-stage asymptomatic to late-stage dementia by means of the patterns of progression of multiple markers, including neuropsychological measures (NMs), magnetic resonance imaging (MRI)-based data and cerebrospinal fluid (CSF) biomarkers.

The diagnosis of CU, MCI or dementia by expert clinicians has traditionally relied on cognitive assessments. However, including multiple domains can help explain and more accurately predict the course of the disease. AD is now perceived as a biological continuum that ranges all the way from normal cognition to dementia (Jack et al., 2018).

https://doi.org/10.1016/j.jneumeth.2022.109581
Received 10 November 2021; Received in revised form 2 March 2022; Accepted 21 March 2022
Available online 25 March 2022

Cognitive decline occurs continuously over a long period, and the progression of biomarker measures is also a continuous process that begins before symptoms. The risk of progression from CU to MCI/dementia depends on a number of factors, including age, sex, and apolipoprotein E (APOE) status (Vermunt et al., 2019). While a number of studies have examined the risk of progression from CU to MCI/dementia at the group level (Soldan et al., 2015; Chen et al., 2017; Parnetti et al., 2019), other authors had used these same measures for predicting progression at the individual level. Multiple investigators had reported predictive models for progression using baseline or longitudinal data and each publication had emphasized a different combination of risk factors and markers. Several groups have attempted to characterize this subtle cognitive impairment using a single cutoff point on a global cognitive domain score (Jack et al., 2012), or with a memory composite score (Vos et al., 2013) or with subtle decline in functional abilities (Edmonds et al., 2015). Recent efforts to improve AD risk prediction have sought to combine sets of variables together that have been linked to symptom onset. These risk prediction approaches have often combined measures associated with CSF biomarkers, hippocampal or entorhinal normalized volume and cognitive test scores (Gavidia-Bovadilla et al., 2017; Gross et al., 2017; Albert et al., 2018; Steenland et al., 2018; van Maurik et al., 2019; Wang et al., 2020; Luo et al., 2021; Palmqvist et al., 2021).

Some studies reviewed automated techniques for classifying and predicting diagnosis using data from different modalities (Zheng et al., 2016; Rathore et al., 2017; Han et al., 2017; Parnetti et al., 2019). While these procedures to assess disease severity are valid for creating a clinical grouping of patients, modeling disease progression by a number of discrete stages is a simplification of a continuous process. AD progression can only be established by repeated evaluations of the patients over time. Longitudinal studies allow the observation of individual patterns of change, providing relevant information that can improve the differential diagnosis (Bernal-Rusiel et al., 2013; Gavidia-Bovadilla et al., 2017; Minhas et al., 2017). A standard strategy for analyzing the association between longitudinal data and the progression to AD is to perform a comparison based on dichotomizing subjects into two clinical groups (Chételat et al., 2005; Moradi et al., 2015; Korolev et al., 2016; Gavidia-Bovadilla et al., 2017), which uses the linear mixed effect (LME) for modeling biomarker trajectories. However, the nature of the estimation problem with regard to AD progression is not dichotomous. To overcome these drawbacks, survival models consider a unique clinical group that takes into account conversion times and finite follow-up or censoring (Kleinbaum and Klein, 2010; Sabuncu et al., 2014). These predictive models can be built by means of the temporal modeling of biomarker trajectories using LME combined with extended Cox survival analysis, which allows the use of exploratory variables that are time dependent (Kleinbaum and Klein, 2010). These approaches allow a coarse approximation of the multivariate features to be used to classify clinical groups.

Recently, a new machine learning framework regards AD progression as a continuous process and derives long-term pathological trajectories from short-term clinical data (Donohue et al., 2014; Guerrero et al., 2016; Schmidt-Richberg et al., 2016; Li et al., 2019; Lorenzi et al., 2019). Long-term disease dynamics are of great interest and importance and have been hypothesized without rigorous methods (Jack et al., 2010; Donohue et al., 2014). Beyond giving a data-driven description of the natural evolution of AD, disease progression models (DPMs) provide automatic diagnosis by explicitly ordering biomarkers from normal to pathological stages along the disease time axis in a multivariate manner. DPM is based on the analysis of longitudinal samples from multiple cohorts at different stages of the disease. A time zero is required to fit the DPM. Age is typically considered a risk factor for developing AD, but age at first diagnosis of AD can vary by decades among patients. A more natural scale for studying the patterns of cognitive decline is time since symptom onset. The time of onset of cognitive impairment might be a candidate time zero. For example, Guerrero et al. (2016) and Schmidt-Richberg et al. (2016) proposed two approaches, which require cohorts with known disease onset. Guerrero et al. (2016) used mixed effects modeling to derive global and individual marker trajectories for a training population, which was later used to instantiate personalized models for unseen subjects. Schmidt-Richberg et al. (2016) proposed a DPM that describes typical trajectories of biomarker values in the course of disease, which were learned using quantile regression. However, the disease onset can be unreliable, the diagnosis is subjective, MCI or dementia are not absorbing states, and reversion to CU diagnoses occurs. An alternative class of DPM relies on the ordering of the observed longitudinal trajectories and extracting the modeling of the temporal progress of the disease. Donohue et al. (2014) model these trajectories based on self-modeling regression. Long-term progression curves for the multiple outcomes and subject-specific random effects and time shifts are estimated iteratively until the convergence of the proposed algorithm, which is called growth models by alternating conditional expectation (GRACE). Li et al. (2019) proposed a latent time joint mixed effects model (LTJMM) for characterizing biomarker trajectories in aging. LTJMM extends joint mixed effects models to include an individual-specific latent time shift. Another approach to DPM in AD is event-based models (Fonteijn et al., 2012; Young et al., 2014; Venkatraghavan et al., 2019), where cutoff points of abnormality are inferred from observed biomarkers, and disease stage is mapped to a discrete set of biomarker abnormality events.

In the present study, we propose a DPM based on the determination of an optimal subset of markers. These optimal measures were selected through a predictive model that uses survival analysis with longitudinal data. Subsequently, the proposed combination of MRI-based data, CSF biomarkers and NMs was used to construct DPMs using GRACE and LTJMM.

2. Materials

The Alzheimer's Disease Neuroimaging Initiative (ADNI) dataset was selected to evaluate the proposed two-stage approach, where subjects made different numbers of visits to the clinic (Wyman et al., 2013). A different number of samples from each subject and markers are available, e.g., not all available time points contain all cognitive, CSF data or imaging information. The inclusion and exclusion criteria, schedule of assessments, and other details can be found at http://adni.loni.usc.edu/. The ADNI is a large-scale multisite study that aims to analyze biomarkers for characterizing the progression of AD. Subjects were recruited from 56 sites in the United States and Canada (Weiner and Veitch, 2015). To date, the ADNI has recruited over 2100 adults, aged between 54 and 92 years, to participate in its four studies (ADNI-1, -GO, −2 and −3). Some ADNI-1 participants are currently followed for more than 10 years. ADNI has developed standardized methods that would allow the comparison of results from multiple centers and scanner-hardware variations within the initiative (Weiner and Veitch, 2015). The ADNI has been used by many publications focused on the characterization of age-related brain changes (Weiner et al., 2013) and early prediction of conversion to probable AD (Moradi et al., 2015; Eskildsen et al., 2015; Korolev et al., 2016; Gavidia-Bovadilla et al., 2017).

The information was extracted from the ADNIMERGE R package (Anon, 2021). We focused on the following assessments: Alzheimer's Disease Assessment-Cognitive 11 and 13-item scale (ADAS11, ADAS13), Clinical Dementia Rating-Sum of Boxes (CDRSB), Mini-Mental State Examination (MMSE), Montreal Cognitive Assessment (MOCA), Rey Auditory Verbal Learning Test Immediate (RAVLT Immediate, Learning, Forgetting, Percent Forgetting), Everyday Cognition (ECog)-total by participant (ECogPtTotal) and study partner (ECogSPTotal) and Functional Assessment Questionnaire (FAQ). Brain imaging measures include volumetric measure summaries of hippocampal, ventricular, entorhinal, and whole brain volumes. These measures were computed with Freesurfer using a cross-sectional processing (v4.3 and 5.1) (https://surfer.nmr.mgh.harvard.edu/).

A second analysis was performed among individuals who also had available beta-amyloid data. Various studies have also examined the association of cognitive impairment with CSF levels of Aβ42, total tau (TAU), phosphorylated tau 181p (pTAU), and the ratio of $TAU/A\beta$ or $pTAU/A\beta$ (Jack et al., 2018; Hansson et al., 2018; Insel et al., 2019). Lumbar puncture was performed as described in the ADNI procedures manual (http://www.adni-info.org/). CSF samples were measured using the Elecsys β-amyloid(1−42) CSF (Bittner et al., 2016), and the Elecsys phosphotau (181 P) CSF and Elecsys total-tau CSF immunoassays on a cobas e 601 analyzer (software version 05.02), according to the preliminary kit manufacturer's instructions and as described in previous studies (Bittner et al., 2016). CSF measures were collected only on a subset of ADNI volunteers, as evidenced by the relative sparsity of CSF data.

To predict CU-to-MCI/dementia conversion, we chose patients diagnosed with CU at their baseline assessments and asked whether their diseases had converted to MCI/dementia during the follow-up of subjects. At each visitation, a clinical diagnosis was made to identify CU subjects whose cognitive decline had converted to probable MCI/dementia according to ADNI clinical assessments (Anon, 2021). For those subjects whose disease progression had converted to MCI or dementia (who were denoted as progression CU, pCU), the conversion time was

Table 1
Baseline demographic and clinical characteristics of the subjects. Data represent the mean (SD) (minimum, maximum) or n (%). The normalized volumes were scaled by 10^3. NHV= normalized hippocampal volume; NMV= normalized medial temporal lobe volume; NEV= normalized entorhinal volume; R-Immediate= RAVLT Immediate;.

Demographic and clinical characteristics						
Feature	MRI+NM			MRI+NM+CSF		
Subjects	316 (sCU)	93 (pCU)	523 (MCI)	218 (sCU)	64 (pCU)	399 (MCI)
Visits	1967 (33.6%)	804 (13.8%)	3086 (52.7%)	1326 (30.9%)	570 (13.3%)	2394 (55.8%)
Female	160 (50.6%)	42 (45.2%)	217 (41.5%)	116 (53.2%)	28 (43.8%)	167 (41.9%)
Age	74.19 (5.80)	76.36 (5.04)	72.29 (7.80)	73.71 (6.02)	76.43 (5.16)	71.67 (7.61)
	56.20–89.60	63.20–89.00	54.40–91.40	56.20–89.60	63.20–89.00	54.40–91.40
Education	16.34 (2.75)	16.02 (2.67)	15.90 (2.88)	16.36 (2.63)	16.00 (2.75)	16.11 (2.73)
	6.00–20.00	8.00–20.00	4.00–20.00	6.00–20.00	8.00–20.00	8.00–20.00)
MRI data						
NHV	4.97 (0.62)	4.58 (0.58)	4.69 (0.78)	5.02 (0.57)	4.63 (0.54)	4.73 (0.79)
	(3.13 6.64)	(3.33 6.02)	(2.66 6.80)	(3.52 6.64)	(3.59 6.02)	(2.66 6.80)
NVV	21.46 (10.78)	24.89 (10.92)	24.50 (13.43)	20.76 (9.75)	25.13 (11.00)	24.06 (13.39)
	(5.67 63.85)	(4.60 63.27)	(4.63 78.63)	(5.67 61.32)	(4.60 63.27)	(4.63 77.60)
NFV	11.84 (1.57)	11.50 (1.60)	11.87 (1.60)	12.17 (1.52)	11.71 (1.52)	12.08 (1.56)
	(8.18 16.47)	(8.00 16.42)	(7.31 17.32)	(8.39 16.47)	(8.00 16.42)	(7.31 17.32)
NMV	13.55 (1.51)	12.96 (1.41)	13.31 (1.62)	13.69 (1.47)	13.04 (1.41)	13.49 (1.60)
	(9.43 18.11)	(9.68 17.53)	(8.76 19.00)	(10.34 18.11)	(9.68 15.91)	(8.76 19.00)
NEV	2.57 (0.37)	2.41 (0.48)	2.41 (0.44)	2.60 (0.35)	2.42 (0.47)	2.44 (0.43)
	(1.64 3.79)	(1.26 3.62)	(1.12 3.76)	(1.64 3.70)	(1.26 3.62)	(1.16 3.76)
Cognitive outcomes						
R-Forgetting	3.57 (2.66)	4.05 (2.67)	4.30 (2.51)	3.55 (2.71)	4.22 (2.72)	4.32 (2.46)
	(−5.00 13.00)	(−2.00 12.00)	(−4.00 13.00)	(−5.00 12.00)	(−2.00 12.00)	(−4.00 13.00)
R-Immediate	45.18 (9.89)	41.40 (9.32)	37.43 (11.11)	46.10 (9.81)	41.02 (9.00)	38.10 (11.11)
	(16.00 71.00)	(22.00 67.00)	(13.00 68.00)	(18.00 71.00)	(22.00 64.00)	(13.00 68.00)
R-Learning	5.94 (2.20)	5.29 (2.60)	4.69 (2.52)	5.93 (2.21)	5.50 (2.51)	4.84 (2.51)
	(0.00 11.00)	(−2.00 11.00)	(−4.00 12.00)	(0.00 11.00)	(0.00 11.00)	(−1.00 12.00)
R-P-Forget	33.43 (27.08)	41.89 (28.23)	51.15 (31.46)	32.76 (28.12)	41.87 (27.03)	50.27 (30.74)
	(−100.00 100.00)	(−20.00 100.00)	(−36.36 100.00)	(−100.00 100.00)	(−20.00 100.00)	(−36.36 100.00)
ADAS11	5.73 (2.84)	7.03 (3.20)	8.66 (3.86)	5.76 (2.92)	7.33 (3.42)	8.36 (3.79)
	(0.00 19.00)	(0.00 17.00)	(1.00 25.33)	(0.00 19.00)	(2.00 17.00)	(1.00 25.33)
ADAS13	8.79 (4.09)	11.12 (4.58)	13.93 (5.85)	8.81 (4.21)	11.33 (4.57)	13.47 (5.79)
	(0.00 23.00)	(1.00 24.00)	(2.00 36.33)	(0.00 23.00)	(3.00 24.00)	(2.00 36.33)
FAQ	0.12 (0.50)	0.29 (0.89)	1.93 (3.02)	0.13 (0.54)	0.33 (0.94)	1.90 (3.11)
	(0.00 5.00)	(0.00 6.00)	(0.00 21.00)	(0.00 5.00)	(0.00 6.00)	(0.00 21.00)
MMSE	29.10 (1.10)	29.02 (1.12)	27.96 (1.75)	29.14 (1.10)	28.94 (1.18)	28.10 (1.72)
	(25.00 30.00)	(24.00 30.00)	(23.00 30.00)	(25.00 30.00)	(24.00 30.00)	(23.00 30.00)
CDRSB	0.03 (0.13)	0.04 (0.13)	1.28 (0.75)	0.03 (0.12)	0.03 (0.12)	1.24 (0.74)
	(0.00 1.00)	(0.00 0.50)	(0.50 5.50)	(0.00 1.00)	(0.00 0.50)	(0.50 5.50)
ADASQ4	2.68 (1.68)	3.54 (1.93)	4.63 (2.27)	2.69 (1.70)	3.50 (1.84)	4.51 (2.27)
	(0.00 9.00)	(0.00 10.00)	(0.00 10.00)	(0.00 9.00)	(0.00 10.00)	(0.00 10.00)
MOCA	25.99 (2.33)	24.57 (2.15)	24.04 (3.05)	26.00 (2.38)	24.73 (2.23)	24.01 (2.98)
	(20.00 30.00)	(19.00 28.00)	(14.00 30.00)	(20.00 30.00)	(19.00 28.00)	(14.00 30.00)
EcogPtTotal	1.32 (0.30)	1.33 (0.28)	1.77 (0.51)	1.31 (0.30)	1.35 (0.27)	1.77 (0.52)
	(1.00 2.49)	(1.00 2.16)	(1.03 3.82)	(1.00 2.49)	(1.00 2.16)	(1.03 3.82)
EcogSPTotal	1.14 (0.20)	1.28 (0.40)	1.60 (0.50)	1.13 (0.17)	1.30 (0.44)	1.60 (0.51)
	(1.00 2.64)	(1.00 2.87)	(1.00 3.47)	(1.00 1.95)	(1.00 2.87)	(1.00 3.47)
CSF biomarkers						
Aβ				1227.14 (441.42)	1073.05 (472.52)	1095.01 (443.04)
				(203.00 1700.00)	(200.00 1700.00)	(210.90 1700.00)
TAU				225.19 (84.78)	274.16 (90.86)	253.62 (123.65)
				(80.00 590.10)	(114.20 462.80)	(97.89 1300.00)
pTAU				20.60 (8.58)	25.64 (9.21)	23.89 (13.38)
				(8.00 59.99)	(9.90 48.27)	(8.21 120.00)
$TAU/A\beta$				0.22 (0.15)	0.33 (0.25)	0.29 (0.24)
				(0.09 1.03)	(0.11 1.61)	(0.07 2.13)
$pTAU/A\beta$				0.02 (0.02)	0.03 (0.03)	0.03 (0.03)
				(0.01 0.12)	(0.01 0.18)	(0.01 0.20)

established between the baseline and the first visit where the patient was diagnosed with MCI/dementia, so long as the diagnosis was reconfirmed on subsequent visits. The stable CU (sCU) group only included CU subjects who were followed up and whose cognitive decline did not convert to probable MCI/dementia. In addition, the last visits of the sCU subjects defined the censorship times. For the first study, i.e. with only NM and MRI data of the subjects, the CU subjects were divided into 316 sCU and 93 pCU subjects according to the clinical follow-up. In the second analysis, i.e. adding CSF markers to MRI measurements and neuropsychological tests, the cohort was established with 218 sCUs and 64 pCUs. Additionally, with the purpose of characterizing the cognitive decline from the selected biomarkers, MCI subjects who did not progress towards dementia in their temporal evolution were also included. For the first and second analyses, 523 and 399 patients were added, respectively. As expected, the number of observations decreases over time from baseline due to attrition and administrative censoring. Summary measures of baseline outcomes for each diagnosis group are presented in Table 1. The value ranges of the markers on the studied clinical groups were consistent with other works that used the ADNI database (Donohue et al., 2014; Moradi et al., 2017; Steenland et al., 2018), and even with other cohorts within the preclinical problem of AD (van Maurik et al., 2019; Wang et al., 2020).

3. Methods

We propose a two-stage approach for the prediction of categorical diagnosis and disease progression modeling. For the first stage, a survival analysis was applied to determine some subsets of the selected multivariate markers from longitudinal data, which allowed discrimination between clinical groups. In the second stage, these subsets of multivariate outcomes were submitted to develop DPMs by means of GRACE and LTJMM approaches.

3.1. Predictive models using survival analysis

Let p markers be measured from n individuals at different follow-up times. We denote the measured outcome k for individual i at time j as y_{ijk}, where $i = 1, \ldots, n$, $k = 1, \ldots, p$ and $j = 1, \ldots, q_{ik}$. A LME model is expressed as:

$$y_{ijk} = x'_{t_{ijk}}\beta_k + \alpha_{0ik} + \alpha_{1ik}t_{ijk} + e_{ijk}$$

where a short-term observation time is represented by t_{ijk}, $x'_{t_{ijk}}$ is the row vector for the fixed effects (including variables such as age and scan time), and β_k are the fixed effects coefficients. In addition to the fixed effects, a mixed effects model is used for subject-specific random effects. The LME models are built with an intercept and slope as random effects to be included in the longitudinal trajectory (Bernal-Rusiel et al., 2013). The parameters α_{0ik} and α_{1ik} are the subject- and outcome-specific random intercept and slope. The vector $(\alpha_{0ik}, \alpha_{1ik})$ follows a bivariate Gaussian distribution with mean zero and covariance matrix $\sum_k$. These values reflect how the subset of regression parameters for the ith subject deviates from those of the population. e_{ijk} is a measurement error term that follows a zero-mean Gaussian distribution with variance σ_k.

Given a population of CU subjects, from which a series of longitudinal measurements were extracted, these outcomes were modeled by LME. Therefore, for each subject, it was possible to estimate the value of each marker over time. In addition, it was also known whether the subject's disease had become MCI or dementia in the follow-up period. For those pCU subjects, the conversion time was calculated from the baseline. Otherwise, i.e. for sCU subjects, the censorship time was also known. An extended Cox model was constructed for each significant discrete time (Platero and Tobar, 2020). The Cox model can be extended for independent and dependent variables over time:

$$h_{ij} = h_j \exp\left(\sum_{k=1}^{p_1}\eta_k \cdot y_{ijk} + \sum_{l=1}^{p_2}\theta_l \cdot z_{il}\right), \quad (1)$$

where h_j is the baseline hazard function, and the first and second terms in the exponential include the effects of p_1 and p_2 time-varying and independent variables $\{y_{ijk}, z_{il}\}$ with associated coefficients $\{\eta_k, \theta_l\}$, respectively. The hazard ratio (HR) quantifies the differential risk of an ith subject characterized by $\{y_{ijk}, z_{il}\}$ in relation to a reference subject characterized by $\{y_{rjk}, z_{rl}\}$ at the same time:

$$HR_{irj} = \frac{h_{ij}}{h_{rj}} = \exp\left(\sum_{k=1}^{p_1}\eta_k(y_{ijk} - y_{rjk}) + \sum_{l=1}^{p_2}\theta_l(z_{il} - z_{rl})\right), \quad (2)$$

where $HR > 1$ indicates that the subject characterized by $\{y_{ijk}, z_{il}\}$ has an increased risk of disease conversion with respect to the reference subject, $\{y_{rjk}, z_{rl}\}$. Conversely, if $HR < 1$, the conversion risk is decreased. In our case, we had three models, i.e. one for the beginning of the study and one each for follow-up at 12 and up to 24 months. To build each of these predictive models, the hazard ratios were calculated and converted into probabilistic terms of conversion from CU to MCI/dementia using the logistic regression model:

$$p_{irj} = \frac{1}{1 + \frac{1}{HR_{irj}}}, \quad (3)$$

where HR_{irj} is the hazard ratio at visit j, ($j \in \{0, 12, 24\}$) and $\{y_{ijk}, z_{il}\}$ and $\{y_{rjk}, z_{rl}\}$ are the vectors of the exploratory variables of the subject and the reference at visit j, respectively. These vectors are formed with p_1 time-varying and p_2 time-independent variables, the latter being modeled by means of LME. HR_{irj} was built by means of an extended Cox-LME model with $\{y_{rjk}, z_{rl}\}$, which was calculated using a random subset of the training population at visit j. This subset was sampled with the same number of subjects representing both sCU and pCU patients. The components of $\{y_{rjk}, z_{rl}\}$ were defined by the average values of this population and scaled by their standard deviations. Therefore, each exploratory variable was defined as a z-score. If a subject with $\{y_{ijk}, z_{il}\}$ shows $HR_{irj} > 1$, then $p_{irj} > 0.5$, and on the contrary, when $HR_{irj} < 1$, then $p_{irj} < 0.5$, where p_{irj} denotes the probability of conversion into MCI/dementia of the disease of subject i at visit j.

3.1.1. Feature selection and building the predictive models

A nested cross-validation (CV) procedure was used to avoid model overfitting and optimistically biased estimates of model performance (Korolev et al., 2016). The procedure consisted of two nested CV loops: an inner loop, designed to select the optimal feature subsets for the proposed models, and an outer loop, designed to obtain an unbiased estimate of model performance. Note that in this manner, double dipping, i.e., using the same data for both feature selection and learning the classifier, was avoided. A nested k-fold CV procedure was applied. The value for k was fixed to 10, a value that was found through experimentation to generally result in a model skill estimate with low bias and modest variance (Kuhn and Johnson 2013). Both the outer and inner CV loops used a 10-fold CV design. In the outer CV loop, the data were partitioned into model and test data (see Fig. 1). In the inner CV loop, the model data were again partitioned into training and validation data.

For each inner CV loop, a set of combinations of markers with different dimensions was proposed, which were subsequently evaluated in the outer CV loop. A feature ordering stage that uses the minimal-redundancy-maximal-relevance (mRMR) algorithm (Peng et al., 2005) to propose good subsets of markers for the prediction of CU conversion was used. Two steps of each inner CV loop were developed with the following activities: (I) A resampling method searched for the first 10 subsets of each dimension that appeared most frequently in mRMR. Feature subsets with dimensions from 1 to 10 were explored. For this purpose, random partitions of training data were subjected to the mRMR algorithm. We used the mutual information difference metric, and the

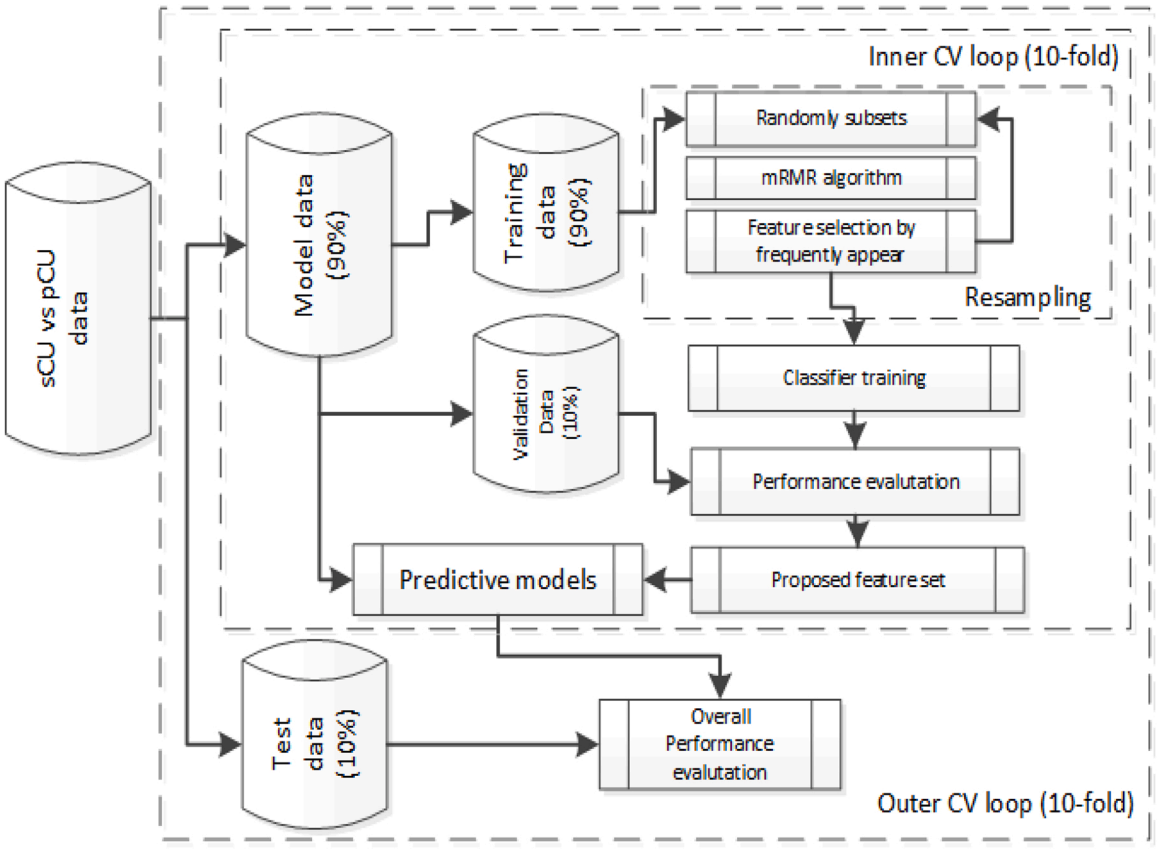

Fig. 1. Nested 10-fold cross-validation procedure for predictive model development and evaluation.

features were normalized to zero mean and unit variance in the mRMR algorithm. This sequence (i.e., partitions of the random subsets of training, applying mRMR and proposing combination features) was repeated 100 times for each inner loop. For each dimension, the 10 combinations of features that most frequently appeared were selected. (II) Predictive models were built using only the training data with the above candidate feature subsets. Of these, the 3 top-performing combinations of markers in terms of classification accuracy determined the evaluation of their corresponding models were selected. Therefore, for each outer iteration, 30 subsets for each dimension were evaluated. In the outer CV loop, for each candidate feature selection, a predictive model was built from the training data, and its performances were evaluated with the withheld test data, which were not used during feature selection, model selection, or final model construction. For better replicability, the nested 10-fold CV procedure was repeated with different partitions of the data, generating multiple performance estimate values. In total, there were 30,000 evaluations of selected subsets for each dimension. Note that these 30,000 proposals for each dimension of the combinations of markers only use training information. For each proposed predictive model, sensitivity, specificity and accuracy scores of the classifiers were computed (Cuingnet et al., 2011). Additionally, receiver operating characteristic (ROC) curves were also calculated. The discriminant value of the corresponding ROC curve was estimated using the area under the curve (AUC). Predictive models with more frequent appearances of the feature subsets (i.e. number of times that the combination of proposed features was evaluated by the CV procedure) and higher classification scores were selected. Fig. 1 shows the general procedure for the development of the predictive models and their subsequent evaluation.

A MATLAB implementation of our method is available at https://www.nitrc.org/projects/twogrsurvana/. The proposed algorithm may generate new predictive models. Faced with a new problem, the subject identifiers, their visits, and a list of proposed markers to be explored must be provided. Note that both the feature selection and the construction of the predictive models do not require tedious parameter adjustment, since mRMR does not require any parameter, nor the modeling of the trajectories with the LME approach, nor do the classification tasks require any parameter.

3.2. Disease progression models

The proposal of Donohue et al. (2014) adds a new component to mixed effects modeling:

$$y_{ijk} = g_k(t^c_{ijk} + \delta_i) + x'_{t^c_{ijk}}\beta_k + \alpha_{0ik} + \alpha_{1ik}t^c_{ijk} + e_{ijk},$$

where g_k is a continuously differentiable monotone function and δ_i is the unknown subject-specific time shift, which has mean zero and variance σ^2_δ. Following the same annotation above, short-term observation time is represented by t^c_{ijk}, which indicates the centered years in relation to the temporal evolution of the visits, $t^c_{ijk} = t_{ijk} - (t_{i_{end}}/2)$, where $i_{end} = \max_k(q_{ik})$. Currently, the long-term progression time is computed from $t^c_{ijk} + \delta_i$. A self-modeling regression model was applied with linear subject-level effects and long-term features with nonparametric monotone smoothing (Donohue et al., 2014). The goal of the algorithm is to estimate both the time shift parameters and the short-term and long-term curves.

Regarding LTJMM, the temporal evolution of the markers is expressed as:

$$y_{ijk} = \gamma_k(t^c_{ijk} + \delta_i) + x'_{t^c_{ijk}}\beta_k + \alpha_{0ik} + \alpha_{1ik}t^c_{ijk} + e_{ijk},$$

the parameter γ_k corresponds to the outcome-specific slope with respect to shifted or long-term time $t^c_{ijk} + \delta_i$. Obviously, the time shift δ_i

quantifies the progression of the i-th individual relative to the population, which is assumed to follow $\delta_i \sim N(0, \sigma_\delta^2)$. The distribution assumptions for random effects are multivariate Gaussian $\alpha_i \sim N(0, \Sigma_\alpha)$. Therefore, GRACE allows different monotonous curve shapes on the long-term trajectories without prespecifying any parametric families, and LTJMM imposes that long-term trajectories must be linear.

Before fitting the DPM approaches to the data, the original values of the outcomes were transformed into percentiles using a weighted empirical cumulative distribution function so that all outcomes were on a common scale. All the outcomes are oriented to be increasing: i.e., the markers of disease progress from normal to abnormal on a common vertical scale. The percentile scale is a natural choice to attain a common scale. The proposed measures were transformed to a percentile scale. The resulting scale was percentile-normalized to range from 0 (least severe observed value) to 1 (most severe observed value). Because the clinical groups are not represented equally, a weighted percentile transformation was used. Percentiles were calculated using the empirical cumulative distribution function, derived by weighting according to the inverse of the proportion of observations from each clinical category. The predicted values on the transformed scale were then transformed back into the original scale. Note that none of these DPMs included clinical groups as a fixed effect.

3.2.1. The onset or time zero

The time shift was assumed to follow $\delta_i \sim N(0, \sigma_\delta^2)$, and t^c_{ijk} was the centered years of the visits. We also note that δ_i is a relative measure of disease progression accounting for the biomarker variabilities observed in the training population. On the other hand, the time of onset should be biased since our populations include more MCI subjects than CU subjects.

For an initial year of cognitive decline or time zero, t_{onset}, the trajectories from sCU subjects should be to the left of t_{onset}, i.e. the markers evolve in negative long-term times. In contrast, for pCU subjects, the marker trajectories should cross t_{onset} towards positive values. Therefore, sensitivity and specificity with the proposed temporal ordering could be measured. Specificity was the percentage of sCU subjects whose last visits, $t^c_{i_{end}} + \delta_i$ where $i_{end} = \max_k(q_{ik})$, had negative times with respect to the total number of sCU subjects:

$$SPE = \frac{\left\{ i \middle| (i \in sCU) \cap ((t^c_{i_{end}} + \delta_i) < t_{onset}) \right\}}{sCU}$$

Regarding sensitivity, two measures were established: (a) the proportion of pCU subjects who at baseline did not have cognitive decline and had negative times, $(t^c_{i_1} + \delta_i) < 0$ where $i_1 = \min_k(q_{ik})$, compared to the total number of pCU subjects:

$$SEN_1 = \frac{\left\{ i \middle| (i \in pCU) \cap ((t^c_{i_1} + \delta_i) < t_{onset}) \right\}}{pCU}$$

and (b) the ratio of pCU subjects whose last visits have positive times with respect to the total number of pCU subjects:

$$SEN_2 = \frac{\left\{ i \middle| (i \in pCU) \cap ((t^c_{i_{end}} + \delta_i) > t_{onset}) \right\}}{pCU}$$

Therefore, a time zero was estimated by means of the maximization of the three previous classification measures.

4. Results

A multivariate analysis was carried out to generate the proposed predictive models. For the study, 5 ROI-based MRI measures of cortical and subcortical structures, 13 NMs and 5 CSF biomarkers were simultaneously considered. Summary measures of baseline outcomes for each diagnosis group are presented in Table 1.

A nested k-fold CV procedure was applied, and the proposed predictive models were built with their subsequent evaluations (see subsection 3.1.1). Categorical predictive models were selected taking into account both their prediction scores and the number of times their feature vectors were proposed to be evaluated. Table 2 summarizes the scores of the predictive models with the two cohorts. Predictive models with more frequent occurrences of the feature subsets (i.e. the number of times the proposed feature combination was evaluated by the CV procedure), higher AUC values and balanced sensitivity and specificity were selected. Several predictive models instead of one for each discrete time were presented due to these proposed models exhibiting combinations of markers with similar performance. Age at baseline was exclusively used as a covariate in LME models for the extended Cox approach. Furthermore, age was also used as a time-independent variable in the survival models.

The classification scores were similar between the two cohorts, as were the combinations of proposed markers to be used to build the predictive models. The normalized hippocampal volume (NHV) and the cognitive and functional scores of ADAS11, FAQ and EcogSPTotal were suggested as measures to be used in the different proposed predictive models. When including the CSF markers, pTAU or the ratio of $pTAU/A\beta$ or $TAU/A\beta$ were also proposed. Over time, the scores improved in both populations, especially from baseline to month 12. By using age, gender and years of education as covariates in the modeling of the trajectories with LME, the scores did not show significant improvements.

Table 3 shows the coefficients associated with the z-score variables of the categorical proposed predictive models at baseline, as well as their significant effects on the progression to MCI/dementia. The minus sign in the coefficient indicates that the marker is a decreasing variable with cognitive decline. Since the variables were normalized into z-scores, the absolute coefficient values indicate the importance of the variables in estimating the clinical prognosis. In both populations, ADAS11 and FAQ were the markers that contributed the most to the classification of cognitive decline. NHV was the third-most important measure, and age was the fourth. When the CSF markers were added, the ratio of $pTAU/A\beta$ had a lower weight; however, its p-value was very low, which makes its contribution significant. Other markers (normalized entorhinal volume-NEV, ECog) were also observed with less influence. However, note that these results correspond to a cross-sectional and marginal analysis of the feature vectors. Instead, the proposed approach was multivariate and longitudinal.

After selecting the marker subsets for each population, the DPM algorithms (GRACE and LTJMM) were applied. The measures were transformed into percentiles. Figs. 2 and 3 show the individual observed trajectories for each marker, in the original scale, ordered in the progression timeline using the two DPM approaches applied. Fig. 2 depicts the first cohort (316 sCU, 93 pCU and 523 sMCI) with only MRI data and NM. The second analysis was performed with a subgroup of the previous population (218 sCU, 64 pCU and 399 sMCI), including subjects who also had measures of CSF markers (see Fig. 3). In both figures, the long-term trajectories were also highlighted in each marker, population and DPM approach. Note that the DPMs were blind to the information of the clinical group of the subjects. Even so, the short-term trajectories were painted with different colors depending on the clinical group of the subjects. This visualization allows observation of the temporal ordering proposed by the DPM algorithms among the subjects according to the diagnostic categorizations. The long-term times were consistent with physician diagnosis.

For a more quantitative evaluation of the predictions of the continuous markers, two performance metrics were used. The first metric was related to the classification of the DPM algorithms in relation to subjects and clinical groups as a function of the long-term time, $t^c_i + \delta_i$. The second metric evaluated the estimation of the conversion times in the pCU subjects. The times of onset of cognitive decline (or time zero values) were established to maximize the classification measures based

Table 2
Scores for predicting CU-to-MCI/dementia conversion using NM+MRI or NM+MRI+CSF. For each visit (Baseline, bl, Month 12, m12, Month 24, m24), a predictive model was built with the extended Cox approach. Numbers within parentheses represent the 95% confidence interval (except for the frequency column). H=Hippocampus (normalized volume); E = Entorhinal (normalized volume); MT=Medial Temporal (normalized volume); A11 =ADAS11; F=FAQ; M=MOCA; EP=EcogPtTotal; ES=EcogSPTotal; PT=pTAU; PTAb=pTAU/Aβ; TAb=TAU/Aβ; AUC=Area under the curve; ACC=Accuracy; SEN=Sensitivity; SPE=Specificity; Frequency=Minimum and maximum range of the number of times that the combination of proposed features was evaluated by the cross-validation procedure.

Data	SEN (%)	SPE (%)	ACC (%)	AUC	Frequency	Optimal feature subsets
$NM + MRI_{bl}$	63.7(62.9 64.6)	64.3(63.8 64.7)	64.1(63.8 64.5)	0.688(0.683 0.693)	742–1512	*H, E, A11, F, EP, ES* *M, E, A11, F, ES* *E, F, EP*
$NM + MRI_{m12}$	77.9(76.9 78.9)	75.0(74.5 75.6)	74.7(74.2 75.1)	0.814(0.808 0.820)	2382–2821	*H, E, F, A11, EP, ES* *E, MT, A11, F, ES* *E, F, EP*
$NM + MRI_{m24}$	74.8(73.7 76.0)	77.3(76.7 77.9)	75.4(74.9 75.9)	0.822(0.814 0.829)	2170–2495	*H, E, F, A11, EP, ES* *H, A11, F, EP* *H, E, A11, F, EP*
$NM + MRI + CSF_{bl}$	64.4(63.6 65.3)	70.9(70.5 71.3)	69.2(68.9 69.6)	0.732(0.727 0.737)	2176–2229	*H, A11, F, M, ES, PT* *A11, F, ES, PTAb* *A11, F, ES, PT*
$NM + MRI + CSF_{m12}$	82.4(81.0 83.7)	71.1(70.2 71.9)	72.3(71.5 73.0)	0.833(0.823 0.842)	2176–2229	*H, A11, ES, TAb* *A11, ES, PTAb* *H, A11, EP, PTAb*
$NM + MRI + CSF_{m24}$	84.3(82.4 86.2)	74.7(73.2 76.2)	75.4(74.2 76.6)	0.854(0.840 0.867)	2176–2229	*H, A11, F, ES, PTAb* *A11, F, ES, TAb* *E, A11, EP, PTAb*

Table 3
Coefficients associated with the markers (in z-score values) of the proposed predictive models at baseline, as well as their significant effects in the progression into MCI/dementia: a) The first subset from MRI data and NMs. b) The second subset from MRI data, NMs and CSF biomarkers. Numbers within parentheses represent the 95% confidence interval. NHV= normalized hippocampal volume; NEV= normalized entorhinal volume.

Marker	coefficient	p-value
NHV	-0.33 (−0.34 −0.33)	0.019 (0.015 0.023)
NEV	-0.10 (−0.11 −0.09)	0.470 (0.377 0.563)
ADAS11	0.41 (0.40 0.41)	0.000 (0.000 0.000)
FAQ	0.29 (0.28 0.30)	0.005 (0.004 0.006)
EcogPtTotal	0.13 (0.12 0.13)	0.189 (0.151 0.226)
EcogSPTotal	0.07 (0.06 0.08)	0.532 (0.427 0.638)
Age	0.25 (0.24 0.25)	0.067 (0.054 0.081)
NHV	-0.30 (−0.31 −0.29)	0.068 (0.054 0.081)
ADAS11	0.48 (0.47 0.49)	0.001 (0.001 0.001)
FAQ	0.47 (0.46 0.48)	0.000 (0.000 0.000)
EcogSPTotal	0.25 (0.26 0.24)	0.111 (0.089 0.133)
pTAU/Aβ	0.25 (0.24 0.26)	0.012 (0.009 0.014)
Age	0.28 (0.28 0.29)	0.082 (0.066 0.099)

on the clinical group of each patient (see subsection 3.2.1). For the first cohort (NM+MRI), the estimated time zero was 1.4 years with GRACE (SEN_1 = 76.3%, SEN_2 = 78.5%, SPE = 76.6%) and 3.6 years with LTJMM (SEN_1 = 80.7%, SEN_2 = 81.8%, SPE = 66.1%). For the second population (NM+MRI+CSF), the estimated time zero was 2.6 years with GRACE (SEN_1 = 79.7%, SEN_2 = 79.7%, SPE = 82.6%) and 2.6 years with LTJMM (SEN_1 = 79, 7%, SEN_2 = 84.4%, SPE = 79.4%) (see supplementary material for further details). With the estimated time of onset, the conversion time in pCU subjects could be measured. This time was defined as the difference between the estimated time onset and the first visit of the patient in the disease timeline, $t_{onset} - (t^c_{i_1} + \delta_i)$. Pearson's correlations were moderate. The values for the first cohort (NM + MRI) were 0.44 (GRACE) and 0.38 (LTJMM), and those of the second population (NM+MRI+CSF) were 0.48 (GRACE) and 0.49 (LTJMM) (see supplementary material for further details). The correlations of the time shifts, δ_i, calculated between GRACE and LTJMM for the patients of the two populations studied was also analyzed. Strong correlations (0.84 and 0.98) between the GRACE and LTJMM approaches for the disease progression time in both populations were also observed (see supplementary material for further details).

One goal of the analysis was to compare the long-term trends in the evolution of the markers on a common scale and to draw conclusions about the proposed temporal order. Figs. 4 and 5 show the long-term progression curves of the outcomes in percentiles. Unlike the LTJMM approach, GRACE allows long-term trends to be nonlinear, i.e., $g_k()$ was assumed to be a continuously differentiable monotone function. Nevertheless, with the exception of the long-term FAQ curve, in GRACE, the long-term curves were close to quasi-linear. From these experimental observations, we suspect that the similarities of the long-term trajectories between the two evaluated DPM approaches were the causes of the high correlations between the estimated progression times of the subjects, for example $t^c_{i_1} + \delta_i$ (see supplementary material for further details). Since the long-term trajectories of the markers were quasi-linear on the common percentage scale, it is relevant to analyze the values of the markers at the beginning of the proposed natural history (about 15 years before the onset of cognitive decline) or intercepts and their annual slopes. Intercepts with high values compared to the rest of the markers would show that this marker is a risk factor in the conversion towards cognitive decline, while the slopes show the speed of the marker in relation to cognitive decline with time. Fifteen years before the onset of cognitive decline, EcogSPTotal presents values of 30% regardless of the studied cohort and the proposed approach. It has a slope of less than 2% per year. The second variable with the greatest variability of decades before cognitive decline was the normalized entorhinal volume in the first population and the $pTAU/A\beta$ ratio when CSF measures were included. Both variables show values of 20% fifteen years before onset and present slopes of 2% per year. ADAS11 and hippocampal volume show very similar trajectories in the two populations and with the two approaches, with values of 15% fifteen years before cognitive decline and with a slope of 3% per year. Age presents the highest slope of all the variables used in both populations and with both approaches: approximately 4% per year. FAQ shows a sigmoid shape in its long-term trends and steep sloping in the transition to cognitive decline.

5. Discussions

In this study, we proposed a two-stage data-driven approach for the prediction of categorical diagnosis and disease progression modeling. We have focused on AD, especially in the early phase, which constitutes a window of opportunity for preventive therapies. The proposed methodology was applied to a population recruited by the ADNI and diagnosed with CU at their baseline assessments, and it was determined

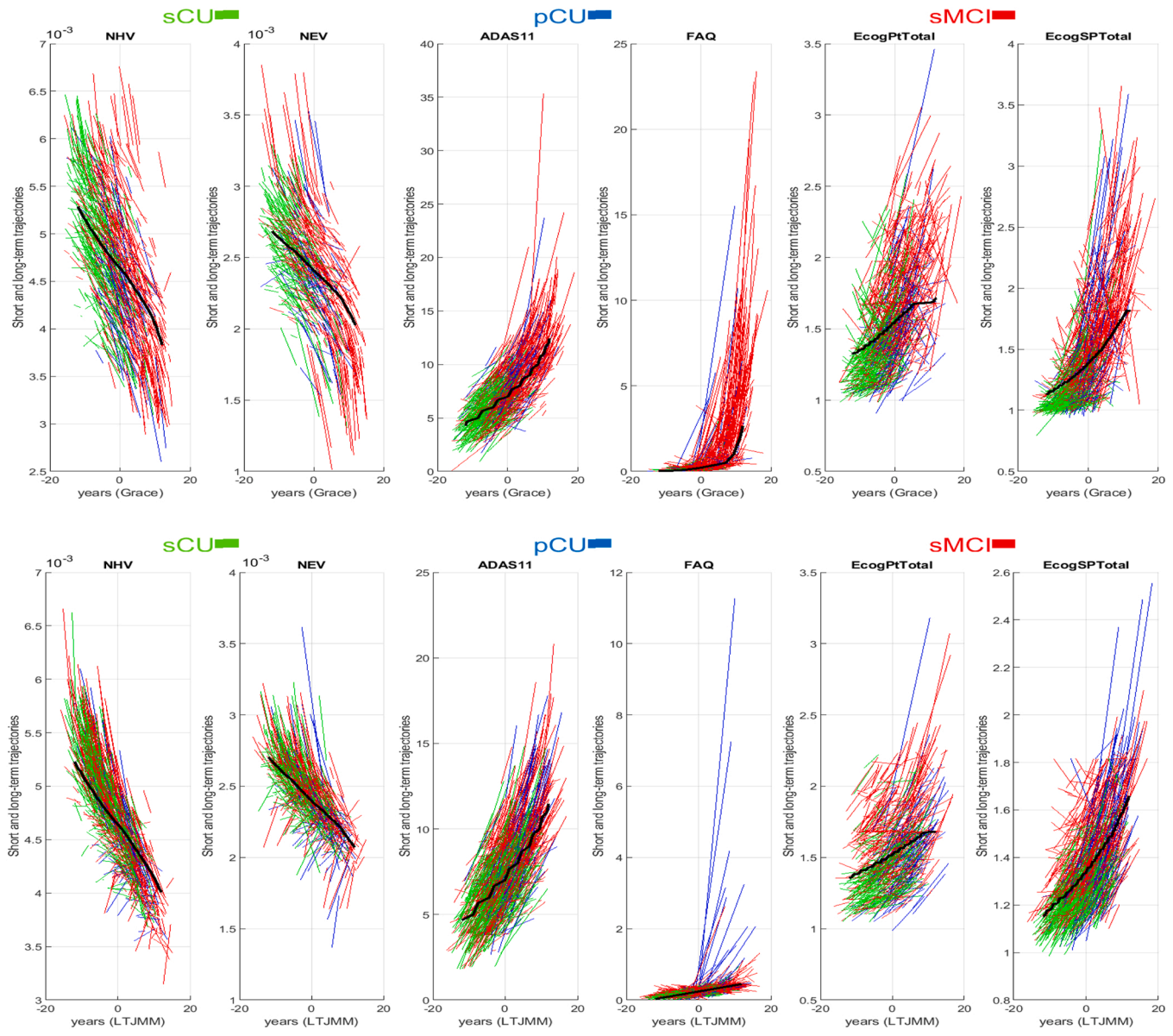

Fig. 2. For the first studied population (MRI data and NMs), the long-term trajectories (black lines) are superimposed over the subject-level observations in the original scale and colored according to diagnosis (sCU in green, pCU in blue and sMCI in red). The first row depicts the trajectories from the GRACE algorithm, and the second row shows the trajectories derived using LTJMM. NHV= normalized hippocampal volume; NEV= normalized entorhinal volume.

whether their diseases had converted to MCI/dementia during the follow-up of subjects. To explore the role of amyloid pathology, we applied our approach to a subset of the original data involving only individuals with amyloid and tau information available by means of CSF biomarkers (see Table 1).

We developed predictive models of CU-to-MCI/dementia progression that combine a very small subset of MRI-based data, CSF markers and standard cognitive measures. These markers are easily interpretable, generating robust, verifiable and reliable predictive models. The predictive models were built using longitudinal data. LME models of the longitudinal trajectories of the markers were used, and the survival analysis only explored the information of the subjects until the conversion or censoring times by means of the extended Cox approach. Feature subsets of different dimensions were preselected using the mRMR algorithm, and a resampling method searched through each dimension for the feature subsets that appeared most frequently. Subsequently, the proposed feature subsets were evaluated in terms of the cross-validated classification accuracy (see Fig. 1, Table 2). The correlation matrices between random intercepts and random slopes from the selected markers show that these measures complement each other, providing additional information to the problem (see supplementary material). This quality is derived from the proposed approach for the feature selection and cross-validation of the predictive models.

Previous studies have evaluated different biomarker combination strategies (Korolev et al., 2016; Gavidia-Bovadilla et al., 2017; Iddi et al., 2019), with the aim of providing a framework for clinical classification and selection of subjects for clinical trials. Evidence that measures of amyloid abnormalities in the brain improve accuracy in detecting cognitive decline has prompted their inclusion as selected biomarkers (Sevigny et al., 2016; Wolz et al., 2016; Bertens et al., 2017). In this direction, it has been suggested that the inclusion of hippocampal volume, together with amyloid positivity, could support the identification of subjects who progress more rapidly to cognitive decline (Wolz et al., 2016). In the two studied populations, both the feature selection for building the predictive models and their classification scores were similar. The inclusion of CSF markers added the $pTAU/A\beta$ ratio, which

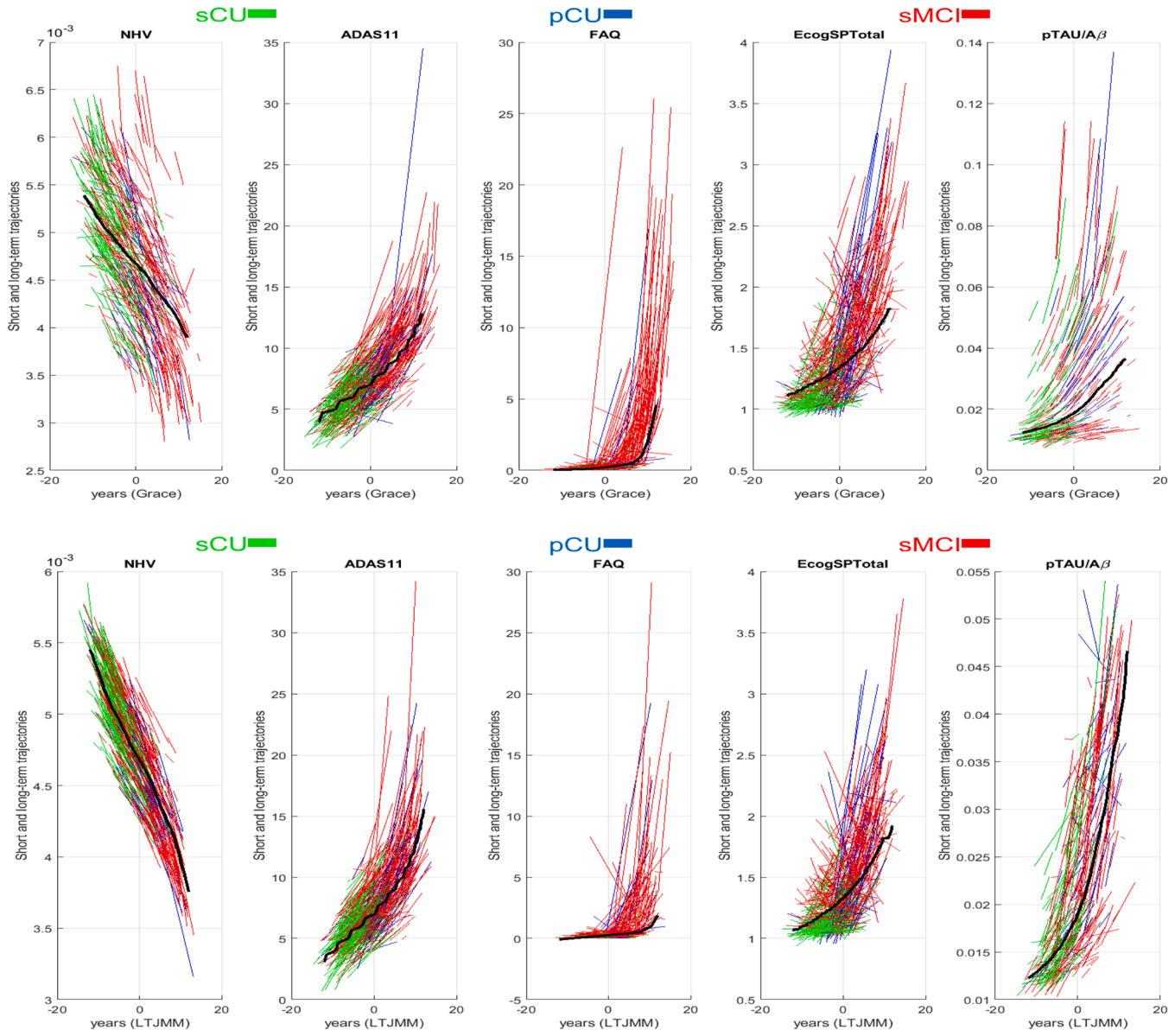

Fig. 3. For the second studied population (MRI data, NMs and CSF biomarkers), the long-term trajectories (black lines) are superimposed over the subject-level observations in the original scale and colored according to diagnosis (sCU in green, pCU in blue and sMCI in red). The first row depicts the trajectories from the GRACE algorithm, and the second row shows the trajectories derived using LTJMM. NHV= normalized hippocampal volume.

slightly improved the classification scores. This measure is well correlated with amyloid PET measurements (Hansson et al., 2018). The selection of $pTAU/A\beta$ over other CSF biomarkers reflects the synergistic effect of tau and amyloid neurodegenerative processes, which were combined into a single diagnostic biomarker (Blennow et al., 2010). This is aligned with recent evidence from a study demonstrating that the CSF $pTAU/A\beta$ ratio had 88% sensitivity and 93% specificity in identifying the presence of amyloid pathologies (Hansson et al., 2018). The selected markers were consistent with previous works. Several authors used different vectors to detect pCU patients. Albert et al. (2018) proposed to combine the Digit Symbol Substitution test, Paired Associates Immediate Recall scores, Aβ, pTAU, right hippocampal volume, right entorhinal cortex thickness and APOE ε4 status. Palmqvist et al. (2021) used the measures of pTAU status (abnormal/normal), number of APOE ε4 alleles, age, education level, and the test scores from the 10-word delayed recall test, Trail-Making test B, and animal fluency. Steenland et al. (2018) combined the hippocampal volume, TAU/Aβ ratio, and summary memory score from the ADAS-Cog, RAVLT, Logical Memory, and MMSE.

Given a selected marker subset of a studied population, DPM approaches reveal the natural history of cognitive decline by ordering the short-term trajectories of the subjects, which are in different stages of AD. The estimated times of disease progression must be validated. In the Results section, the time zero was estimated from the clinical classification of the patients. Another way to calculate the time zero could be by means of the definition of the preclinical AD. At this stage, subjects present, at least, Aβ positivity (Jack et al., 2018). The $pTAU/A\beta$ ratio is highly concordant with PET classification and predicted clinical progression (Hansson et al., 2018). Values above 0.028 indicate positive results for amyloid. The cutoff for $pTAU/A\beta$ was defined against 18 F-florbetapir PET in ADNI (Hansson et al., 2018). Considering the long-term trajectory of the $pTAU/A\beta$ ratio for the population with CSF biomarkers and using the threshold of 0.028, the time zero values were 6.4 and 5.3 years according to the GRACE and LTJMM approaches, respectively. For the time zero values estimated according to the clinical classification of the patients, the $pTAU/A\beta$ values were 0.023 in year 2.6 using the GRACE approach and 0.024 in year 3.6 with LTJMM.

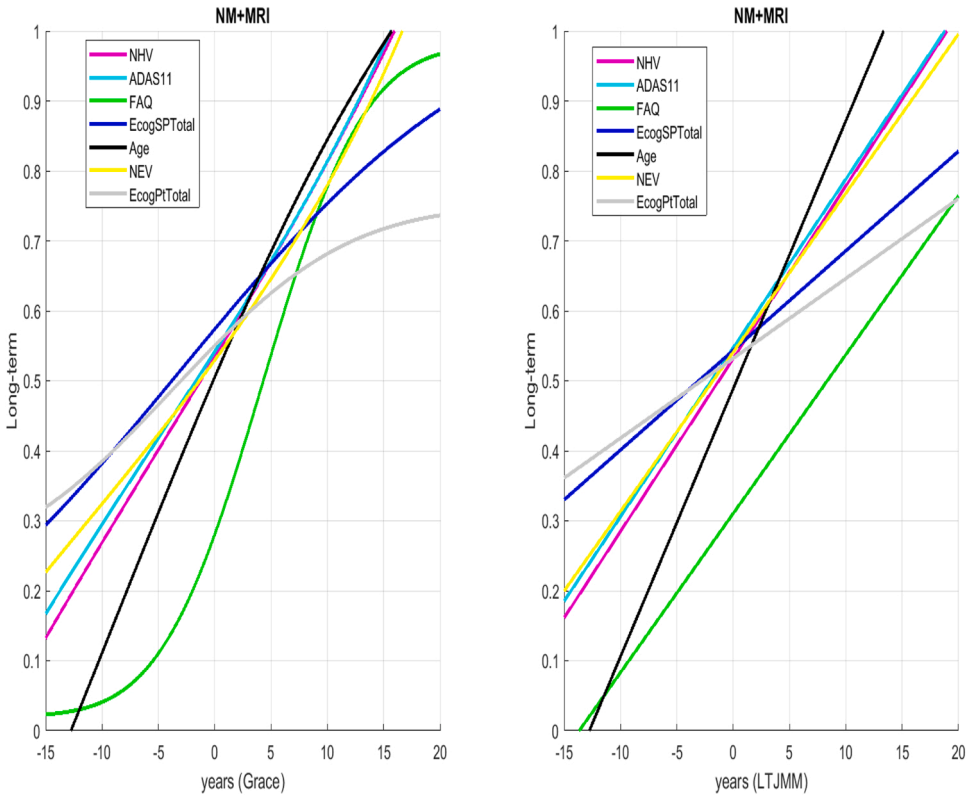

Fig. 4. For the first studied population (MRI data and NMs), long-term progression curves of the outcomes in percentiles according to the applied DPM approach: a) GRACE (left), b) LTJMM (right).

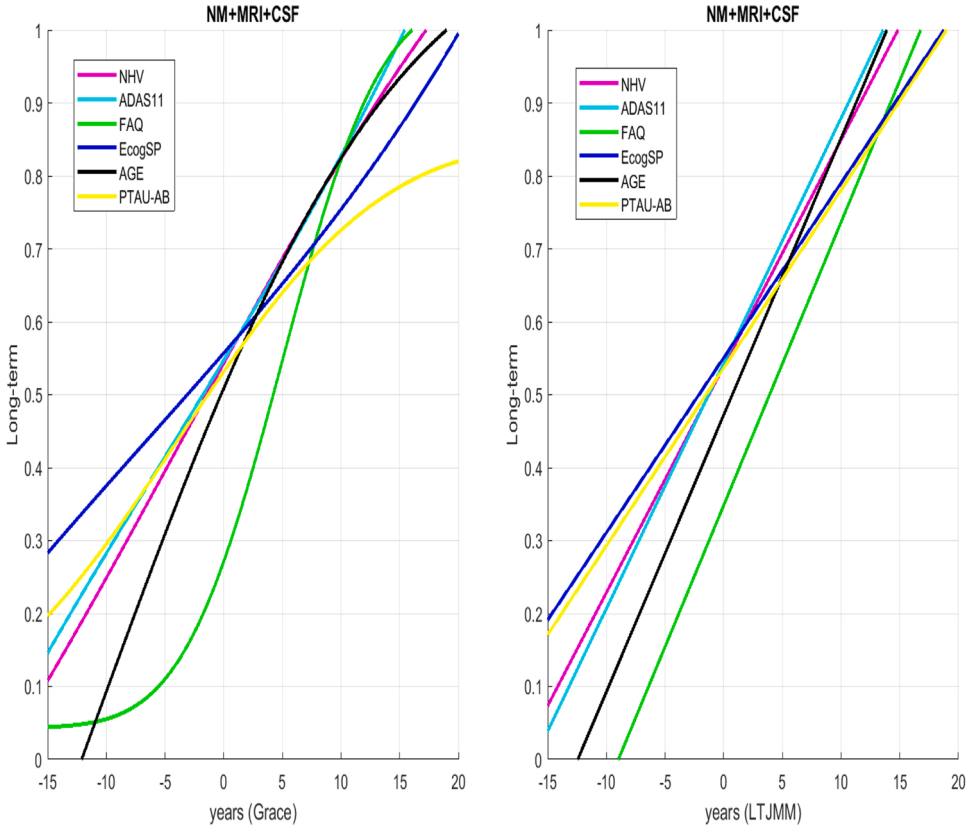

Fig. 5. For the second studied population (MRI data, NMs and CSF biomarkers), long-term progression curves of the outcomes in percentiles according to the applied DPM approach: a) GRACE (left), b) LTJMM (right).

GRACE allows different monotonous curve shapes on the long-term trajectories without prespecifying any parametric families. LTJMM imposes that long-term trajectories must be linear. Here, in most of the selected markers, all trajectories tend to track very closely to each other in near-linear trajectories in GRACE, except for FAQ (see Figs. 4 and 5). These results are in line with those already indicated by Donohue et al. (2014). As a consequence, the high correlation between the time shifts, δ_i, obtained by GRACE and LTJMM is well explained (see supplementary material for further details). On the other hand, the GRACE estimates of the time shifts, δ_i, of the common subjects between the two studied populations tended to be very similar. Therefore, the long-term trajectories of the proposed markers shared between the two cohorts were also very similar. Greater discrepancies were found in the estimates of δ_i with LTJMM (see Fig. 6). This means that the estimates of δ_i from GRACE were more robust than those produced using LTJMM, since the long-term trajectories maintained similar tracks even when changing part of the population and with some different markers.

Based on both the high correlation of δ_i between the common subjects of the two populations with different vectors, as well as the similarity of the trends of the long-term trajectories between the common markers, which is especially true with GRACE, we could conclude that, at least in the early stage, CSF biomarkers do not make significant contributions in the predictive models and DPMs of the clinical scheme, although their inclusion slightly improves both the categorical classification results and the correlation between the conversion times of the pCU subjects and their estimates using the DPM algorithms. In any case, the current trend would be to use NMs in predictive models and DPMs for the evolution of clinical symptoms and to use CSF biomarkers for the quantification of neuropathological processes, both in amyloid and tau pathology as well as in the neurodegenerative process.

Table 3 shows the weights of the selected markers at baseline for the classification between the clinical categories of sCU or pCU. A striking difference is observed in how the proposed markers first become abnormal along the disease time axis (see Figs. 4 and 5). Although FAQ and ADAS11 were the markers that most contributed to the classification of cognitive decline (see Table 3), the $pTAU/A\beta$ ratio, everyday cognition and the volume of the entorhinal cortex showed alterations of more than 20% fifteen years before the onset of cognitive decline. Apart from the $pTAU/A\beta$ ratio, which has already been discussed, the other two markers require some additional comments. Although functional impairment was thought to occur only after cognitive decline, studies suggest that subtle functional impairment occurs even in cognitively normal individuals who then progress to MCI or dementia (Weintraub et al., 2018). The ECog scale is an assessment tool for daily function that independently queries the patient and an informant about everyday functional capacities in six domains (Farias et al., 2008). Informant-based ratings on the ECog have been shown to be associated with objective measures of disease status, although self-reports may also have sensitivity in the early phase (Rueda et al., 2015). Informant-rated ECog scores are also strongly associated with the risk of progression from MCI to dementia (Lau et al., 2015). Structural MRI studies in subjects diagnosed with AD or MCI consistently show atrophy in the entorhinal cortex and hippocampus, thus gaining a broad consensus that atrophy of the medial temporal lobe (MTL) is the first MRI sign of emerging AD (Tan et al., 2014). In fact, the MTL appears to be the earliest site of AD-related tau accumulation, with tangles initially appearing in the transentorhinal and entorhinal cortex and hippocampus (Soldan et al., 2015). The entorhinal cortex was the most sensitive brain region and brain structure, which changed at the earliest stages during the process of AD initiation and had a maximal atrophy rate in comparison with the hippocampus and amygdala (Miller et al., 2015; Zhou et al., 2016). Furthermore, atrophy in the entorhinal cortex occurred earlier than the clinical manifestation at approximately 8–10 years and even before hippocampal and amygdalar atrophy appeared (Younes et al., 2014; Miller et al., 2015).

5.1. Limitations and future works

Although both the proposed methodology for the constructions of DPMs as well as their evaluation criteria were novel, however, the

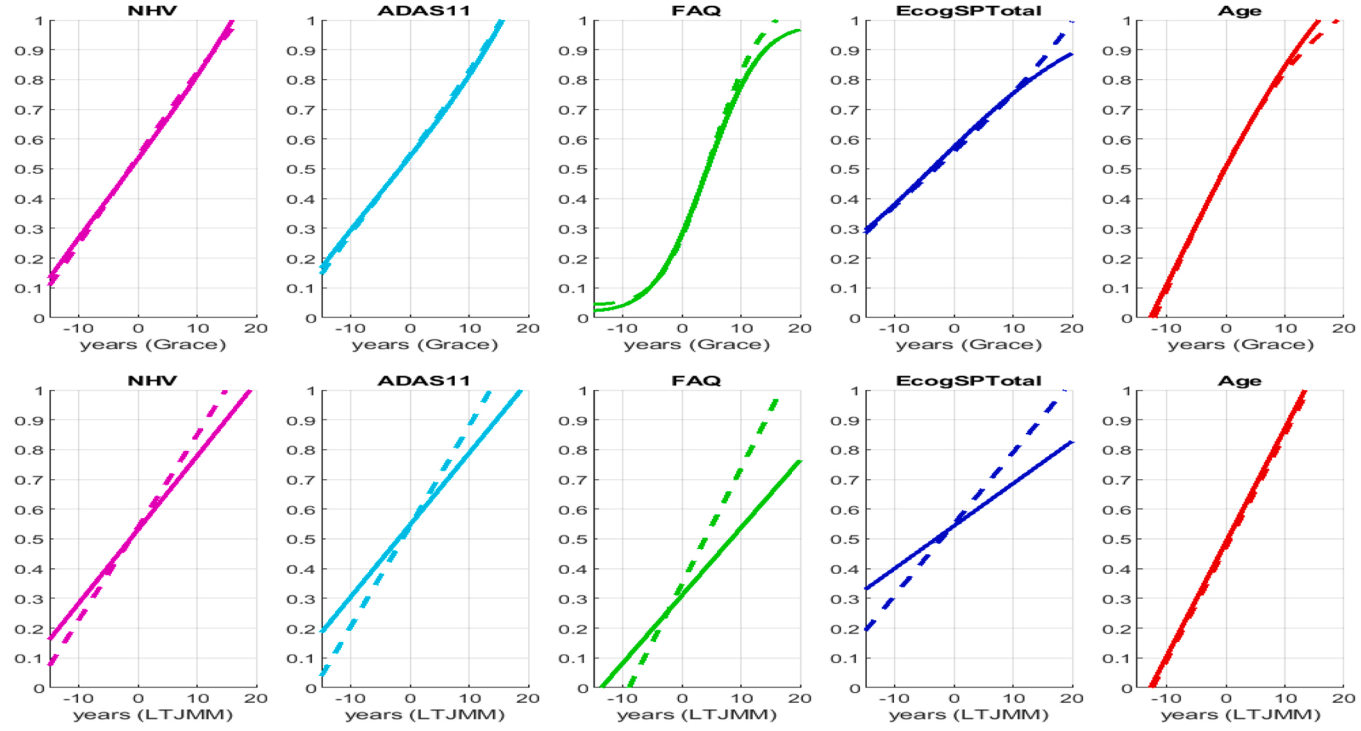

Fig. 6. Temporal evolution of the long-term trajectories, on the percentile scale, of the common markers between the two studied populations. A solid line shows the long-term trajectory of the population with MRI and NM data. The dashed line shows the trajectories of the population that also have CSF measures. The first row shows the long-term trajectories extracted with GRACE. In the second row, the trajectories appear by means of LTJMM.

moderate linear correlation between the conversion times of the pCU subjects and the times estimated by the approaches require further analysis of new vectors. Note that the fixation of the marker vector determines the natural history of disease progression. In addition, given that predictive models and DPMs analyze the temporal evolution of clinical symptoms, while CSF biomarkers are those that characterize the type of neuropathological disorder in cognitive decline, a new line of future work is proposed. A double quantification system will process the transition from CU to MCI/dementia: (a) The detection of amyloid and tau pathologies by means the use of CSF biomarkers, and, (b) Predictive models and DPMs would explain the degree of cognitive decline, mainly through the use of neuropsychological measures.

The modeling of short-term trajectories in both predictive models and DPM approaches was based on linear functions, i.e., using LME models. Nonlinear modeling of the short-term trajectories could reduce the mean absolute error of markers and improve the predictions (Ishida et al., 2019). Additionally, the information on the conversion and censorship times of the subjects in the process of cognitive decline could be considered in the DPM algorithms. In this sense, the estimation of the time shift of each subject, δ_i, in the disease timeline could be improved by including this information.

The progression of AD is affected by multiple factors. Including these factors as covariates in the DPM approaches would allow us to analyze whether the progression of AD would accelerate in some subgroups of the population. In this regard, the influence of sex or APOE genotype on the trends of the long-term trajectories of the selected markers should be explored (Ishida et al., 2019).

Finally, the results of the predictive models and DPMs should be compared when changing the criteria for the selection of subjects belonging to the studied population. Cognitive clinical groups were used here. Considering only CU or MCI subjects with amyloid pathology could result in less variability in the temporal evolution of the markers. This hypothesis should be addressed in the development of new predictive models and DPM related to the evolution of AD.

6. Conclusions

The selection of a set of markers that reliably detects the evolution of Alzheimer's disease is a challenge. These measures will allow us to focus on the affected population, improving the effectiveness of clinical trials. Additionally, given the selected markers, their acquisition, the construction of categorical predictive models or DPMs, and the study of the effects of the covariates could be improved. However, the heterogeneity of the disease presents a major problem for its temporal modeling. This work intended to select a set of measures capable of capturing the diversity of the cognitive decline change in AD. In this study, we proposed a two-stage data-driven approach for the prediction of categorical diagnosis and disease progression modeling. We developed categorical predictive models of CU-to-MCI/dementia progression that combine a very small subset of MRI-based data, CSF markers and standard cognitive measures. The normalized entorhinal and hippocampal volumes, the cognitive and functional scores of ADAS11, FAQ and EcogSPTotal and the ratio of $pTAU/A\beta$ were suggested as measures to be used in the different proposed predictive models. After selecting the marker subsets, the DPM algorithms (GRACE and LTJMM) were applied. The long-term times were consistent with physician diagnosis. The estimates of time shifts, δ_i, from GRACE were more robust than those produced using LTJMM. The ratio of $pTAU/A\beta$, EcogSPTotal and the normalized volume of the entorhinal cortex show alterations of more than 20% fifteen years before the onset of cognitive decline.

CRediT authorship contribution statement

Carlos Platero: Conceptualization, Methodology, Software, Validation, Writing – original draft preparation, Writing – review & editing, Visualization, Investigation.

Declarations of interest

The author declares that the research was conducted in the absence of any commercial or financial relationships that could be construed as a potential conflict of interest.

Acknowledgments

Data collection for this study was funded by the ADNI (National Institutes of Health Grant U01 AG024904). ADNI is funded by the National Institute on Aging, the National Institute of Biomedical Imaging and Bioengineering and through generous contributions from the following: Alzheimer's Association; Alzheimer's Drug Discovery Foundation; BioClinica, Inc.; Biogen Idec Inc.; Bristol-Myers Squibb Company; Eisai Inc.; Elan Pharmaceuticals, Inc.; Eli Lilly and Company; F. Hoffmann-La Roche Ltd and its affiliated company Genentech, Inc.; GE Healthcare; Innogenetics, N.V.; IXICO Ltd.; Janssen Alzheimer Immunotherapy Research & Development, LLC.; Johnson & Johnson Pharmaceutical Research & Development LLC.; Medpace, Inc.; Merck & Co., Inc.; Meso Scale Diagnostics, LLC.; NeuroRx Research; Novartis Pharmaceuticals Corporation; Pfizer Inc.; Piramal Imaging; Servier; Synarc Inc.; and Takeda Pharmaceutical Company. Data used in preparation of this article were obtained from the Alzheimer's Disease Neuroimaging Initiative (ADNI) database (adni.loni.usc.edu). As such, the investigators within the ADNI contributed to the design and implementation of ADNI and/or provided data but did not participate in analysis or writing of this report. A complete listing of ADNI investigators can be found at: http://adni.loni.usc.edu/wp-content/uploads/how_to_apply/ADNI_Acknowledgement_List.pdf.

Appendix A. Supporting information

Supplementary data associated with this article can be found in the online version at doi:10.1016/j.jneumeth.2022.109581.

References

Hyman, B.T., Phelps, C.H., Beach, T.G., Bigio, E.H., Cairns, N.J., Carrillo, M.C., Dickson, D.W., Duyckaerts, C., Frosch, M.P., Masliah, E., et al., 2012. National Institute on Aging-Alzheimeras Association guidelines for the neuropathologic assessment of Alzheimeras disease. Alzheimer Dement. 8, 1–13.

Price, J.L., McKeel Jr., D.W., Buckles, V.D., Roe, C.M., Xiong, C., Grundman, M., Hansen, L.A., Petersen, R.C., Parisi, J.E., Dickson, D.W., et al., 2009. Neuropathology of nondemented aging: presumptive evidence for preclinical Alzheimer disease. Neurobiol. Aging 30, 1026–1036.

Nelson, P.T., Alafuzoff, I., Bigio, E.H., Bouras, C., Braak, H., Cairns, N.J., Castellani, R.J., Crain, B.J., Davies, P., Tredici, K.D., et al., 2012. Correlation of Alzheimer disease neuropathologic changes with cognitive status: a review of the literature. J. Neuropathol. Exp. Neurol. 71, 362–381.

Sperling, R.A., Rentz, D.M., Johnson, K.A., Karlawish, J., Donohue, M., Salmon, D.P., Aisen, P., 2014. The A4 study: stopping AD before symptoms begin? Sci. Transl. Med. 6, 228fs13-228fs13.

Baker, J.E., Lim, Y.Y., Pietrzak, R.H., Hassenstab, J., Snyder, P.J., Masters, C.L., Maruff, P., 2017. Cognitive impairment and decline in cognitively normal older adults with high amyloid-β: a meta-analysis. Alzheimer Dement.: Diagn., Assess. Dis. Monit. 6, 108–121.

Insel, P.S., Weiner, M., Mackin, R.S., Mormino, E., Lim, Y.Y., Stomrud, E., Palmqvist, S., Masters, C.L., Maruff, P.T., Hansson, O., et al., 2019. Determining clinically meaningful decline in preclinical Alzheimer disease. Neurology 93, e322–e333.

Jack Jr., C.R., Bennett, D.A., Blennow, K., Carrillo, M.C., Dunn, B., Haeberlein, S.B., Holtzman, D.M., Jagust, W., Jessen, F., Karlawish, J., et al., 2018. NIA-AA Research Framework: Toward a biological definition of Alzheimeras disease. Alzheimer Dement. 14, 535–562.

Vermunt, L., Sikkes, S.A., Van Den Hout, A., Handels, R., Bos, I., Van Der Flier, W.M., Kern, S., Ousset, P.J., Maruff, P., Skoog, I., et al., 2019. Duration of preclinical, prodromal, and dementia stages of Alzheimeras disease in relation to age, sex, and APOE genotype. Alzheimer Dement. 15, 888–898.

Soldan, A., Pettigrew, C., Lu, Y., Wang, M.C., Selnes, O., Albert, M., Brown, T., Ratnanather, J.T., Younes, L., Miller, M.I., et al., 2015. Relationship of medial temporal lobe atrophy, APOE genotype, and cognitive reserve in preclinical Alzheimer's disease. Hum. Brain Mapp. 36, 2826–2841.

Chen, Y., Denny, K.G., Harvey, D., Farias, S.T., Mungas, D., DeCarli, C., Beckett, L., 2017. Progression from normal cognition to mild cognitive impairment in a diverse clinic-based and community-based elderly cohort. Alzheimer Dement. 13, 399–405.

Parnetti, L., Chipi, E., Salvadori, N., D'Andrea, K., Eusebi, P., 2019. Prevalence and risk of progression of preclinical Alzheimer's disease stages: a systematic review and meta-analysis. Alzheimer Res. Ther. 11, 1–13.
Jack Jr., C.R., Knopman, D.S., Weigand, S.D., Wiste, H.J., Vemuri, P., Lowe, V., Kantarci, K., Gunter, J.L., Senjem, M.L., Ivnik, R.J., et al., 2012. An operational approach to National Institute on Aging-Alzheimer's Association criteria for preclinical Alzheimer disease. Ann. Neurol. 71, 765–775.
Vos, S.J., Xiong, C., Visser, P.J., Jasielec, M.S., Hassenstab, J., Grant, E.A., Cairns, N.J., Morris, J.C., Holtzman, D.M., Fagan, A.M., 2013. Preclinical Alzheimer's disease and its outcome: a longitudinal cohort study. Lancet Neurol. 12, 957–965.
Edmonds, E.C., Delano-Wood, L., Galasko, D.R., Salmon, D.P., Bondi, M.W., 2015. Subtle cognitive decline and biomarker staging in preclinical Alzheimer's disease. J. Alzheimer's Dis. 47, 231–242.
Gavidia-Bovadilla, G., Kanaan-Izquierdo, S., Mataró-Serrat, M., Perera-Lluna, A., A.D.N.I, et al., 2017. Early prediction of Alzheimer's disease using null longitudinal model-based classifiers. PloS One 12, e0168011.
Gross, A.L., Hassenstab, J.J., Johnson, S.C., Clark, L.R., Resnick, S.M., Kitner-Triolo, M., Masters, C.L., Maruff, P., Morris, J.C., Soldan, A., et al., 2017. A classification algorithm for predicting progression from normal cognition to mild cognitive impairment across five cohorts: The preclinical AD consortium. Alzheimer Dement.: Diagn., Assess. Dis. Monit. 8, 147–155.
Albert, M., Zhu, Y., Moghekar, A., Mori, S., Miller, M.I., Soldan, A., Pettigrew, C., Selnes, O., Li, S., Wang, M.C., 2018. Predicting progression from normal cognition to mild cognitive impairment for individuals at 5 years. Brain 141, 877–887.
Steenland, K., Zhao, L., John, S.E., Goldstein, F.C., Levey, A., Alvaro, A., Initiative, A.D.N., et al., 2018. A 'framingham-like' algorithm for predicting 4-year risk of progression to amnestic mild cognitive impairment or Alzheimer's disease using multidomain information. J. Alzheimer's Dis. 63, 1383–1393.
van Maurik, I.S., Slot, R.E., Verfaillie, S.C., Zwan, M.D., Bouwman, F.H., Prins, N.D., Teunissen, C.E., Scheltens, P., Barkhof, F., Wattjes, M.P., et al., 2019. Personalized risk for clinical progression in cognitively normal subjects–the ABIDE project. Alzheimer Res. Ther. 11, 1–9.
Wang, Z., Tang, Z., Zhu, Y., Pettigrew, C., Soldan, A., Gross, A., Albert, M., 2020. AD risk score for the early phases of disease based on unsupervised machine learning. Alzheimer Dement. 16, 1524–1533.
Luo, W., Wen, H., Ge, S., Tang, C., Liu, X., Lu, L., 2021, Development of a sex-specific risk scoring system for predicting cognitive normal to mild cognitive impairment (srss-cnmci).
Palmqvist, S., Tideman, P., Cullen, N., Zetterberg, H., Blennow, K., Dage, J.L., Stomrud, E., Janelidze, S., Mattsson-Carlgren, N., Hansson, O., 2021. Prediction of future Alzheimer's disease dementia using plasma phospho-tau combined with other accessible measures. Nat. Med. 27, 1034–1042.
Zheng, C., Xia, Y., Pan, Y., Chen, J., 2016. Automated identification of dementia using medical imaging: a survey from a pattern classification perspective. Brain Inform. 3, 17–27.
Rathore, S., Habes, M., Iftikhar, M.A., Shacklett, A., Davatzikos, C., 2017. A review on neuroimaging-based classification studies and associated feature extraction methods for Alzheimeras disease and its prodromal stages. NeuroImage 155, 530–548.
Han, S.D., Nguyen, C.P., Stricker, N.H., Nation, D.A., 2017. Detectable neuropsychological differences in early preclinical Alzheimer's disease: A meta-analysis. Neuropsychol. Rev. 27, 305–325.
Bernal-Rusiel, J.L., Greve, D.N., Reuter, M., Fischl, B., Sabuncu, M.R., A.D.N.I, et al., 2013. Statistical analysis of longitudinal neuroimage data with linear mixed effects models. Neuroimage 66, 249–260.
Minhas, S., Khanum, A., Riaz, F., Khan, S., Alvi, A., 2017. Predicting progression from mild cognitive impairment to Alzheimeras disease using autoregressive modelling of longitudinal and multimodal biomarkers. IEEE J. Biomed. Health Inform.
Chételat, G., Landeau, B., Eustache, F., Mézenge, F., Viader, F., de La Sayette, V., Desgranges, B., Baron, J.C., 2005. Using voxel-based morphometry to map the structural changes associated with rapid conversion in MCI: a longitudinal MRI study. Neuroimage 27, 934–946.
Moradi, E., Pepe, A., Gaser, C., Huttunen, H., Tohka, J., A.D.N.I, et al., 2015. Machine learning framework for early MRI-based Alzheimer's conversion prediction in MCI subjects. Neuroimage 104, 398–412.
Korolev, I.O., Symonds, L.L., Bozoki, A.C., A.D.N.I, et al., 2016. Predicting progression from mild cognitive impairment to Alzheimer's dementia using clinical, MRI, and plasma biomarkers via probabilistic pattern classification. PloS One 11, e0138866.
Kleinbaum, D.G., Klein, M., 2010. Survival Analysis. Volume 3. Springer.
Sabuncu, M.R., Bernal-Rusiel, J.L., Reuter, M., Greve, D.N., Fischl, B., A.D.N.I, et al., 2014. Event time analysis of longitudinal neuroimage data. NeuroImage 97, 9–18.
Donohue, M.C., Jacqmin-Gadda, H., LeGoff, M., Thomas, R.G., Raman, R., Gamst, A.C., Beckett, L.A., Jack Jr., C.R., Weiner, M.W., Dartigues, J.F., et al., 2014. Estimating long-term multivariate progression from short-term data. Alzheimer Dement. 10, S400–S410.
Guerrero, R., Schmidt-Richberg, A., Ledig, C., Tong, T., Wolz, R., Rueckert, D., ADNI, A.D.N.I., et al., 2016. Instantiated mixed effects modeling of Alzheimeras disease markers. NeuroImage 142, 113–125.
Schmidt-Richberg, A., Ledig, C., Guerrero, R., Molina-Abril, H., Frangi, A., Rueckert, D., Initiative, A.D.N., et al., 2016. Learning biomarker models for progression estimation of Alzheimer's disease. PloS One 11.
Li, D., Iddi, S., Thompson, W.K., Donohue, M.C., Initiative, A.D.N., 2019. Bayesian latent time joint mixed effect models for multicohort longitudinal data. Stat. Methods Med. Res. 28, 835–845.
Lorenzi, M., Filippone, M., Frisoni, G.B., Alexander, D.C., Ourselin, S., Initiative, A.D.N., et al., 2019. Probabilistic disease progression modeling to characterize diagnostic uncertainty: application to staging and prediction in Alzheimeras disease. NeuroImage 190, 56–68.
Jack Jr., C.R., Knopman, D.S., Jagust, W.J., Shaw, L.M., Aisen, P.S., Weiner, M.W., Petersen, R.C., Trojanowski, J.Q., 2010. Hypothetical model of dynamic biomarkers of the Alzheimer's pathological cascade. Lancet Neurol. 9, 119–128.
Fonteijn, H.M., Modat, M., Clarkson, M.J., Barnes, J., Lehmann, M., Hobbs, N.Z., Scahill, R.I., Tabrizi, S.J., Ourselin, S., Fox, N.C., et al., 2012. An event-based model for disease progression and its application in familial Alzheimeras disease and Huntingtonas disease. NeuroImage 60, 1880–1889.
Young, A.L., Oxtoby, N.P., Daga, P., Cash, D.M., Fox, N.C., Ourselin, S., Schott, J.M., Alexander, D.C., 2014. A data-driven model of biomarker changes in sporadic Alzheimeras disease. Brain 137, 2564–2577.
Venkatraghavan, V., Bron, E.E., Niessen, W.J., Klein, S., Initiative, A.D.N., et al., 2019. Disease progression timeline estimation for Alzheimeras disease using discriminative event based modeling. NeuroImage 186, 518–532.
Wyman, B.T., Harvey, D.J., Crawford, K., Bernstein, M.A., Carmichael, O., Cole, P.E., Crane, P.K., DeCarli, C., Fox, N.C., Gunter, J.L., et al., 2013. Standardization of analysis sets for reporting results from ADNI MRI data. Alzheimer Dement. 9, 332–337.
Weiner, M.W., Veitch, D.P., 2015. Introduction to special issue: overview of Alzheimeras Disease Neuroimaging Initiative. Alzheimer Dement. 11, 730–733.
Weiner, M.W., Veitch, D.P., Aisen, P.S., Beckett, L.A., Cairns, N.J., Green, R.C., Harvey, D., Jack, C.R., Jagust, W., Liu, E., et al., 2013. The Alzheimeras Disease Neuroimaging Initiative: a review of papers published since its inception. Alzheimer Dement.: J. Alzheimer Assoc. 9, e111–e194.
Eskildsen, S.F., Coupé, P., Fonov, V.S., Pruessner, J.C., Collins, D.L., 2015. Structural imaging biomarkers of Alzheimer's disease: predicting disease progression. Neurobiol. Aging 36, S23–S31.
Anonthe ADNI team: ADNIMERGE: Alzheimer's Disease Neuroimaging Initiative. (2021) R package version 0.0.1.
Hansson, O., Seibyl, J., Stomrud, E., Zetterberg, H., Trojanowski, J.Q., Bittner, T., Lifke, V., Corradini, V., Eichenlaub, U., Batrla, R., et al., 2018. CSF biomarkers of Alzheimeras disease concord with amyloid-β PET and predict clinical progression: a study of fully automated immunoassays in BioFINDER and ADNI cohorts. Alzheimer Dement. 14, 1470–1481.
Bittner, T., Zetterberg, H., Teunissen, C.E., Ostlund Jr., R.E., Militello, M., Andreasson, U., Hubeek, I., Gibson, D., Chu, D.C., Eichenlaub, U., et al., 2016. Technical performance of a novel, fully automated electrochemiluminescence immunoassay for the quantitation of β-amyloid (1-42) in human cerebrospinal fluid. Alzheimer Dement. 12, 517–526.
Donohue, M.C., Sperling, R.A., Salmon, D.P., Rentz, D.M., Raman, R., Thomas, R.G., Weiner, M., Aisen, P.S., et al., 2014. The preclinical Alzheimer cognitive composite: measuring amyloid-related decline. JAMA Neurol. 71, 961–970.
Moradi, E., Hallikainen, I., Hänninen, T., Tohka, J., Initiative, A.D.N., et al., 2017. Reyas Auditory Verbal Learning Test scores can be predicted from whole brain MRI in Alzheimeras disease. NeuroImage: Clin. 13, 415–427.
Platero, C., Tobar, M.C., 2020. Longitudinal survival analysis and two-group comparison for predicting the progression of mild cognitive impairment to Alzheimer's disease. J. Neurosci. Methods 341, 108698.
Kuhn, M., Johnson, K., 2013. Applied Predictive Modeling, Volume 26. Springer.
Peng, H., Long, F., Ding, C., 2005. Feature selection based on mutual information criteria of max-dependency, max-relevance, and min-redundancy. IEEE Trans. Pattern Anal. Mach. Intell. 27, 1226–1238.
Cuingnet, R., Gerardin, E., Tessieras, J., Auzias, G., Lehéricy, S., Habert, M.O., Chupin, M., Benali, H., Colliot, O., Initiative, A.D.N., et al., 2011. Automatic classification of patients with Alzheimeras disease from structural MRI: a comparison of ten methods using the ADNI database. neuroimage 56, 766–781.
Iddi, S., Li, D., Aisen, P.S., Rafii, M.S., Thompson, W.K., Donohue, M.C., 2019. Predicting the course of Alzheimeras progression. Brain Inform. 6, 1–18.
Sevigny, J., Suhy, J., Chiao, P., Chen, T., Klein, G., Purcell, D., Oh, J., Verma, A., Sampat, M., Barakos, J., 2016. Amyloid PET screening for enrichment of early-stage Alzheimer disease clinical trials. Alzheimer Dis. Assoc. Disord. 30, 1–7.
Wolz, R., Schwarz, A.J., Gray, K.R., Yu, P., Hill, D.L., Initiative, A.D.N., et al., 2016. Enrichment of clinical trials in MCI due to AD using markers of amyloid and neurodegeneration. Neurology 87, 1235–1241.
Bertens, D., Tijms, B.M., Vermunt, L., Prins, N.D., Scheltens, P., Visser, P.J., Initiative, A.D.N., et al., 2017. The effect of diagnostic criteria on outcome measures in preclinical and prodromal alzheimeras disease: implications for trial design. Alzheimer Dement.: Transl. Res. Clin. Interv. 3, 513–523.
Blennow, K., Hampel, H., Weiner, M., Zetterberg, H., 2010. Cerebrospinal fluid and plasma biomarkers in Alzheimer disease. Nat. Rev. Neurol. 6, 131–144.
Weintraub, S., Carrillo, M.C., Farias, S.T., Goldberg, T.E., Hendrix, J.A., Jaeger, J., Knopman, D.S., Langbaum, J.B., Park, D.C., Ropacki, M.T., et al., 2018. Measuring cognition and function in the preclinical stage of Alzheimeras disease. Alzheimer Dement.: Transl. Res. Clin. Interv. 4, 64–75.
Farias, S.T., Mungas, D., Reed, B.R., Cahn-Weiner, D., Jagust, W., Baynes, K., DeCarli, C., 2008. The measurement of everyday cognition (ECog): scale development and psychometric properties. Neuropsychology 22, 531.
Rueda, A.D., Lau, K.M., Saito, N., Harvey, D., Risacher, S.L., Aisen, P.S., Petersen, R.C., Saykin, A.J., Farias, S.T., Initiative, A.D.N., et al., 2015. Self-rated and informant-rated everyday function in comparison to objective markers of Alzheimeras disease. Alzheimer Dement. 11, 1080–1089.
Lau, K.M., Parikh, M., Harvey, D.J., Huang, C.J., Farias, S.T., 2015. Early cognitively-based functional limitations predict loss of independence in instrumental activities of daily living in older adults. J. Int. Neuropsychol. Soc.: JINS 21, 688.

Tan, C.C., Yu, J.T., Tan, L., 2014. Biomarkers for preclinical Alzheimeras disease. J. Alzheimer Dis. 42, 1051–1069.
Miller, M.I., Ratnanather, J.T., Tward, D.J., Brown, T., Lee, D.S., Ketcha, M., Mori, K., Wang, M.C., Mori, S., Albert, M.S., et al., 2015. Network neurodegeneration in Alzheimeras disease via MRI based shape diffeomorphometry and high-field atlasing. Front. Bioeng. Biotechnol. 3, 54.
Zhou, Y., Tan, C., Wen, D., Sun, H., Han, W., Xu, Y., 2016. The biomarkers for identifying preclinical Alzheimeras disease via structural and functional magnetic resonance imaging. Front. Aging Neurosci. 8, 92.
Younes, L., Albert, M., Miller, M.I., Team, B.R., et al., 2014. Inferring changepoint times of medial temporal lobe morphometric change in preclinical Alzheimeras disease. NeuroImage: Clin. 5, 178–187.
Ishida, T., Tokuda, K., Hisaka, A., Honma, M., Kijima, S., Takatoku, H., Iwatsubo, T., Moritoyo, T., Suzuki, H., Initiative, A.D.N., 2019. A novel method to estimate long-term chronological changes from fragmented observations in disease progression. Clin. Pharmacol. Ther. 105, 436–447.